Proceedings of the 1993 IEEE/RSJ International Conference on Intelligent Robots and Systems Yokohama, Japan July 26-30, 1993

The Effect of Payload Impact on the Dynamics of a Space Robot*

Xavier Cyril†, Gilbert J. Jaar‡ and Arun K. Misra‡

Abstract

~~In this paper~~ The effect of payload collision on the dynamics of a spacecraft-manipulator system is studied. To simulate the post-impact dynamics of the spacecraft-manipulator-payload system, initial conditions are derived from the payload impact model. The dynamical model for the post-impact dynamics ~~are~~ is derived using Lagrangian formulation, ~~The formulation is carried out~~ by writing Lagrange's equations for the individual bodies, and then assembling them to obtain the constrained dynamical equations of the system. The non-working constraint wrenches are then eliminated by using the *natural orthogonal complement* which produces a set of independent dynamical equations. Simulation ~~of~~ two impact scenarios ~~are carried out and their results~~ are presented.

+ the

no ital

Results for

1 Introduction

Space manipulators will play an increasingly significant role in future space operations. They will be used for assembly and fabrication of space structures required for the construction of the Space Station. Shuttle-mounted manipulators or other free flying robots will be used for inspection, repair or retrieval of malfunctioning satellites. Berthing of two spacecraft (e.g. Shuttle to the Space Station) could also take place through a manipulator. Many dynamics and control issues must be resolved before the above mentioned operations can become routine. This paper addresses one such issue, that is, the post-impact dynamics associated with the capture of a payload by a spacecraft-mounted manipulator.

The different phases of capturing a payload are: approach (chase) the payload; initial contact (impact) with or without payload rebound; capture process (in the case of space station arm - insert the grapple fixture, latch to the payload and rigidize the interconnection); and finally to suppress any residual motion of the payload. In [1] the authors have studied the dynamics and control of a spacecraft-manipulator system capturing a tumbling satellite, where the phase two of capture was assumed to be a smooth contact, i.e., no impact loading. In this paper we investigate the effect of including the impact loading on the dynamics response.

There is very little available in the literature on the collision dynamics of manipulators. In [2] the authors have studied the modelling of impact on a single flexible arm and in [3] the authors describe a modelling scheme for collision dynamics of space robots.

2 Formulation of the Problem

In this section the dynamical equations of the system will be derived using the Lagrangian formulation. Contrary to the usual practice in Lagrangian dynamics, where the equations for the system as a whole are derived, the Lagrange equations are derived here for each body and then assembled to obtain the equations of motion for the system. This method, however, introduces the non-working constraint wrenches which will be eliminated by using the *natural orthogonal complement* [4].

The system under investigation is illustrated in Figure 1. It is composed of a main body (hereafter referred to as spacecraft) that serves as a platform on which a two-link robotic manipulator is mounted and a payload. It is important to note that although the manipulator shown consists of two links the formulation developed is applicable to N-link manipulator.

If we represent the system under investigation as an N-body system then the vector containing it's independent generalized coordinates (ψ) can be defined as:

$$\psi = [\psi_1^T, \psi_2^T, ..., \psi_N^T]^T \tag{1}$$

where ψ_1 represents the spacecraft's attitude degrees of freedom, namely, pitch, roll, and yaw. It can be written as :

$$\psi_1 = [\alpha, \beta, \gamma]^T \tag{2}$$

For the remaining $N-1$ bodies, the generalized coordinates depend on whether the body is *rigid* or *flexible*.

$$flexible \qquad \psi_i = [\theta_i, \mathbf{b}_i]^T \tag{3}$$

$$rigid \qquad \psi_i = [\theta_i] \tag{4}$$

where

$$\mathbf{b}_i = [b_{i1}, b_{i2}, ..., b_{im}] \tag{5}$$

contains the m generalized coordinates associated with bending in link i, and θ_i is the angle between X_i and X_{i-1} under rigid body conditions (i,e., prior to the deformation of the flexible links), measured along the positive direction of Z_i (Figure 1).

The system shown in Figure 1 consists of 4-bodies. The orbital and system frames are located at the spacecraft's centre of mass C_S. At a given instant in time, the orientation of the body fixed frame (X_1, Y_1, Z_1) relative to the orbital frame (X_0, Y_0, Z_0) defines the spacecraft's attitude, represented by the pitch, roll, and yaw angles. The angular velocity of the orbital frame with respect to the inertial frame (X_I, Y_I, Z_I) located at the Earth's centre, is denoted by Ω.

Let $\mathbf{r}_i$ be the position vector of any point $\mathcal{P}$ on the *flexible* body with respect to (X_i, Y_i, Z_i). A set of unit vectors $\mathbf{x}_i, \mathbf{y}_i, \mathbf{z}_i$ are chosen to be parallel to (X_i, Y_i, Z_i), respectively and x_i, y_i, z_i are the coordinates of a point in the frame. Vector $\mathbf{r}_i$ could be written as

$$\mathbf{r}_i = x_i\mathbf{x}_i + \mathbf{u}_i(x_i, t) \tag{6}$$

where $\mathbf{u}_i$ is the displacement vector due to the bending of body i. The *flexible* links are modelled as *Euler-Bernoulli* beams. The stiffening effect due to the axial shortening is ignored since the links will be moved at low speeds. The deformations of the *flexible* link are described by appropriate modal shape functions and time-dependent generalized coordinates. The displacement vector $\mathbf{u}_i$ can be written in the compact form :

$$\mathbf{u}_i(x_i, t) = \mathbf{B}(x_i)\mathbf{b}_i(t) \tag{7}$$

where $\mathbf{B}_i$ is the matrix of shape functions associated with bending of link i.

*This work was carried out at McGill University.

†Space Systems Engineering, CAE Electronics Ltd., P.O.Box 1800, St.Laurent, Canada H4L 4X4

‡Dept. of Mechanical Engineering, McGill University, Montreal, Canada H3A 2K6

0-7803-0823-9/93/$3.00 (C) 1993 IEEE

The rotation of the tip of link i with respect to (X_i, Y_i, Z_i) due to the flexibility is denoted by $\boldsymbol{\delta}_i$ (Figure 2). The position of the origin of (X_i, Y_i, Z_i) with respect to that of (X_0, Y_0, Z_0) is given by :

$$\mathbf{p}_i = \mathbf{p}_{i-1}(l_{i-1}) + \mathbf{r}_i(l_{i-1}) \tag{8}$$

The angular velocity of (X_i, Y_i, Z_i) with respect to (X_0, Y_0, Z_0) can be shown to be:

$$\boldsymbol{\omega}_i = \boldsymbol{\omega}_{i-1} + \dot{\boldsymbol{\delta}}_{i-1} + \dot{\theta}_i \mathbf{z}_i \tag{9}$$

The kinetic energy of body i, denoted as T_i can be written in the form :

$$T_i = T_i(\mathbf{q}_i, \mathbf{v}_i) = \frac{1}{2}\mathbf{v}_i^T \mathbf{M}_i(\mathbf{q}_i, t)\mathbf{v}_i \tag{10}$$

where $\mathbf{M}_i$ is the *extended inertia matrix* of the dynamical system. Here *extended* refers to quantities which comprise both rotational and translational variables or parameters of the body.

The *extended position vector*, $\mathbf{q}_i$, is defined as:

$$\textit{flexible} \quad \mathbf{q}_i = [\mathbf{p}_i^T, \hat{\mathbf{q}}_i^T, \mathbf{b}_i^T]^T \tag{11}$$

$$\textit{rigid} \quad \mathbf{q}_i = [\mathbf{p}_i^T, \hat{\mathbf{q}}_i^T]^T \tag{12}$$

where $\hat{\mathbf{q}}_i$ is the *quaternion* representing the orientation of body i-fixed frame.

The *extended velocity vector*, $\mathbf{v}_i$ is defined as :

$$\textit{flexible} \quad \mathbf{v}_i = [\dot{\mathbf{p}}_i^T, \boldsymbol{\omega}_i^T, \dot{\mathbf{b}}_i^T]^T \tag{13}$$

$$\textit{rigid} \quad \mathbf{v}_i = [\dot{\mathbf{p}}_i^T, \boldsymbol{\omega}_i^T]^T \tag{14}$$

The potential energy for body i, denoted by U_i, is a function of the *extended position vector* $\mathbf{q}_i$ alone. It consists of two parts; one due to the gravity gradient and the other due to the elastic strain energy stored in the *flexible* body. The effect of the former is much smaller than the latter and is neglected here. Hence the potential energy for a *rigid* body is equal to zero.

The dynamical equations of motion of body i can be derived using the Lagrangian formulation, which is given by the following expression:

$$\frac{d}{dt}\left(\frac{\partial T_i}{\partial \dot{\mathbf{q}}_i}\right) - \frac{\partial T_i}{\partial \mathbf{q}_i} = \boldsymbol{\chi}_i - \frac{\partial U_i}{\partial \mathbf{q}_i} \tag{15}$$

where $\boldsymbol{\chi}_i$ contains the dissipative, external, and constraint forces on body i.

Upon assembling the equations of motion for each body, the system's constrained equations of motion can be written in the form :

$$\mathbf{M}\dot{\mathbf{v}} = \boldsymbol{\phi}^E + \boldsymbol{\phi}^S + \boldsymbol{\phi}^C \tag{16}$$

where

$$\mathbf{M} = \mathrm{diag}(\mathbf{M}_1, \mathbf{M}_2, ..., \mathbf{M}_n) \tag{17}$$

is the generalized extended inertia matrix and $\dot{\mathbf{v}}$, $\boldsymbol{\phi}^E, \boldsymbol{\phi}^S$, and $\boldsymbol{\phi}^C$, represent the generalized extended velocity vector, and the generalized external, system and constraint forces of the system, respectively.

The *natural orthogonal complement*, $\mathbf{N}$, is defined as the matrix which transforms the independent generalized velocities to extended velocities and is obtained from

$$\mathbf{v} = \mathbf{N}(\dot{\boldsymbol{\psi}} + \dot{\boldsymbol{\psi}}_0) \tag{18}$$

where $\dot{\boldsymbol{\psi}}$ is the generalized velocity vector of the system and $\dot{\boldsymbol{\psi}}_0$ is the vector containing the orbital rate Ω of the system. It was proven [4] that upon the pre-multiplication of equation (16) by $\mathbf{N}^T$ the constraint force vector $\boldsymbol{\phi}^C$ could be eliminated. Furthermore, an expression for $\dot{\mathbf{v}}$ is obtained as follows

$$\dot{\mathbf{v}} = \mathbf{N}\ddot{\boldsymbol{\psi}} + \dot{\mathbf{N}}(\dot{\boldsymbol{\psi}} + \dot{\boldsymbol{\psi}}_0) \tag{19}$$

where

$$\dot{\boldsymbol{\psi}}_0 = [\Omega, 0, ..., 0] \tag{20}$$

Upon pre-multiplication of equation (16) by $\mathbf{N}^T$ and the substitution of equation (19), the independent dynamical equation of motion of the system becomes:

$$\tilde{\mathbf{M}}\ddot{\boldsymbol{\psi}} = \mathbf{c}(\boldsymbol{\psi}, \dot{\boldsymbol{\psi}}, \dot{\boldsymbol{\psi}}_0) + \mathbf{f} \tag{21}$$

where

$$\begin{aligned} \tilde{\mathbf{M}} &= \mathbf{N}^T\mathbf{M}\mathbf{N} \\ \mathbf{c} &= \mathbf{N}^T[\boldsymbol{\phi}^S - \mathbf{M}\dot{\mathbf{N}}(\dot{\boldsymbol{\psi}} + \dot{\boldsymbol{\psi}}_0)] \\ \mathbf{f} &= \mathbf{N}^T\boldsymbol{\phi}^E \end{aligned}$$

In the above equation, $\tilde{\mathbf{M}}$ is the generalized mass matrix of the system, which is symmetric and positive definite. Vector $\mathbf{f}$ represents the generalized external forces, and the vector $\mathbf{c}$ contains the Coriolis, damping, and centrifugal terms.

It is more convenient for simulation and control to partition equation (21) into rotational and elastic coordinates dependent matrices and vectors as follows

$$\begin{bmatrix} \tilde{\mathbf{M}}_{\theta\theta} & \tilde{\mathbf{M}}_{\theta b} \\ \tilde{\mathbf{M}}_{b\theta} & \tilde{\mathbf{M}}_{bb} \end{bmatrix} \begin{bmatrix} \ddot{\boldsymbol{\theta}} \\ \ddot{\mathbf{b}} \end{bmatrix} = \begin{bmatrix} \mathbf{c}_\theta \\ \mathbf{c}_b \end{bmatrix} + \begin{bmatrix} \boldsymbol{\tau} \\ \mathbf{0} \end{bmatrix} \tag{22}$$

where the subscripts θ and b represent matrices and vectors related to the rotational and bending degrees of freedom, respectively. The upper part of the external generalized forces vector is equal to $\boldsymbol{\tau}$ which corresponds to the nominal joint torques. The lower part, however, is noted to be equal to zero, which implies that actuators are only present at the joints and separate generalized forces cannot be applied to control the *flexible* modes.

3 Capture of a Payload

We now determine the initial conditions for the post-impact simulation. Let us suppose that a payload (rigid body) with mass M_p and inertia $\mathbf{I}_p$ collides with the end effector of the manipulator with an initial translational velocity $\mathbf{w}_p$ and angular velocity $\boldsymbol{\omega}_p$. During the collision the equations of motion for the spacecraft-manipulator system and the payload can be written as follows:

$$\tilde{\mathbf{M}}\ddot{\boldsymbol{\psi}} = \mathbf{c} + \mathbf{f} + \mathbf{J}^T\mathbf{f}_p \tag{23}$$

$$\mathbf{M}_p\dot{\mathbf{v}}_p = \mathbf{c}_p(\mathbf{v}_p) - \mathbf{A}\mathbf{f}_p \tag{24}$$

where $\mathbf{v}_p$ is the 6-dimensional velocity vector of the payload and $\mathbf{f}_p$ is the generalized force vector due to impact at the instant of collision between the payload and the spacecraft-manipulator system. Vector $\mathbf{c}_p$ contains the velocity and position dependent terms such as Coriolis, damping and centrifugal terms. $\mathbf{M}_p$ and $\mathbf{A}$ are defined as:

$$\mathbf{M}_p = \begin{bmatrix} \mathbf{1}M_p & \mathbf{0} \\ \mathbf{0} & \mathbf{I}_p \end{bmatrix} \tag{25}$$

and

$$\mathbf{A} = \begin{bmatrix} \mathbf{1} & \mathbf{0} \\ -\mathbf{R}_{bc} & \mathbf{1} \end{bmatrix} \tag{26}$$

where $\mathbf{R}_{bc}$ is the cross-product tensor of $\mathbf{r}_{bc}$, which represents the position vector of the payload's centre of mass as measured from the point of contact.

The $(6 \times N')$ Jacobian $\mathbf{J}$ of the system can be written as:

$$\mathbf{J} = \begin{bmatrix} \mathbf{J}_1 \\ \mathbf{J}_2 \end{bmatrix} \tag{27}$$

$$\mathbf{J}_1 = \left[\frac{\partial \mathbf{p}_h}{\partial \psi_1} \cdots \frac{\partial \mathbf{p}_h}{\partial \psi_{N'}} \right] \tag{28}$$

$$\mathbf{J}_2 = [\mathbf{e}_1 \ldots \mathbf{e}_{N'}] \tag{29}$$

where N' is the total number of degrees of freedom in the system, $\mathbf{p}_h$ represents the position vector of the manipulator's end-effector with respect to body-1 frame and $\mathbf{e}_i$ represents the unit vector along the axis of rotation if the i-th degree of freedom is rotational and is zero for the case of elastic degree of freedom.

Upon pre-multiplying equation (24) by $\mathbf{J}^T\mathbf{A}^{-1}$ and adding the result to equation (23) the following is obtained:

$$\mathbf{J}^T\mathbf{A}^{-1}\mathbf{M}_p\dot{\mathbf{v}}_p + \tilde{\mathbf{M}}\ddot{\boldsymbol{\psi}} = \mathbf{c} + \mathbf{J}^T\mathbf{A}^{-1}\mathbf{c}_p + \mathbf{f} \tag{30}$$

Next, equation (30) is integrated over the period of the impact $\mathcal{T}$ with the assumption that there are no joint torques applied during impact i.e., $\mathbf{f} = \mathbf{0}$. The resulting equation after integration is as follows:

$$\mathbf{J}^T\mathbf{A}^{-1}\mathbf{M}_p(\mathbf{v}_{pf} - \mathbf{v}_{pi}) + \tilde{\mathbf{M}}(\dot{\boldsymbol{\psi}}_f - \dot{\boldsymbol{\psi}}_i) = \int_0^{\mathcal{T}} (\mathbf{c} + \mathbf{J}^T\mathbf{A}^{-1}\mathbf{c}_p)dt \tag{31}$$

The impact force $\mathbf{f}_p$ during a collision between two bodies is usually very large and acts for a very short impact time of $\mathcal{T}$. Thus, one can say that

$$\begin{aligned} \mathcal{T} &= \mathcal{O}(\epsilon), \epsilon << 1 && (32) \\ \dot{\boldsymbol{\psi}}, \mathbf{v}_p, \boldsymbol{\psi}, \mathbf{r}_{bc} &= \mathcal{O}(1) && (33) \\ \ddot{\boldsymbol{\psi}}, \dot{\mathbf{v}}_p &= \mathcal{O}(\frac{1}{\epsilon}) && (34) \end{aligned}$$

Clearly, the left-hand side of equation (31) is $\mathcal{O}(1)$. The integrated $\mathbf{c} + \mathbf{J}^T\mathbf{A}^{-1}\mathbf{c}_p$ on the right-hand side is also $\mathcal{O}(1)$; however, the value of the integral is $\mathcal{O}(\epsilon)$ and can be ignored. Thus equation (31) holds good with the right-hand side set equal to zero.

The formulation developed here could be applied to all kinds of collisions ranging from plastic to elastic. In the case of plastic the payload is rigidly attached to the end effector of the manipulator and in the case of elastic the payload rebounds with no loss of energy. However, of interest is the case where the payload is successfully captured (plastic case) and the consequent behaviour of the spacecraft-manipulator system. In such a case the extended velocity vector of the payload after impact $\mathbf{v}_{pf}$ could be written in terms of $\mathbf{J}, \mathbf{R}_{bc}$ and $\dot{\boldsymbol{\psi}}_f$ as follows:

$$\mathbf{v}_{pf} = \tilde{\mathbf{J}}\dot{\boldsymbol{\psi}}_f \tag{35}$$

where

$$\tilde{\mathbf{J}} = \begin{bmatrix} \mathbf{J}_1 + \mathbf{R}_{bc}\mathbf{J}_2 \\ \mathbf{J}_2 \end{bmatrix} \tag{36}$$

Upon substituting of equation (35) into equation (31) and re-arranging the following is obtained:

$$\dot{\boldsymbol{\psi}}_f = \mathbf{G}^{-1}\mathbf{H} \tag{37}$$

where

$$\begin{aligned} \mathbf{G} &= \mathbf{J}^T\mathbf{A}^{-1}\mathbf{M}_p\tilde{\mathbf{J}} + \tilde{\mathbf{M}} && (38) \\ \mathbf{H} &= \mathbf{J}^T\mathbf{A}^{-1}\mathbf{M}_p\mathbf{v}_{pi} + \tilde{\mathbf{M}}\dot{\boldsymbol{\psi}}_i && (39) \end{aligned}$$

from which the angular velocities of the joints and velocities of the elastic coordinates after impact could be solved for in terms of the initial conditions just before impact, i.e., $\mathbf{v}_{pi}$ and $\dot{\boldsymbol{\psi}}_i$. These could then be used as the initial conditions for the post-impact dynamical simulation of the system. Equation (37) looks similar in form to that obtained in [3], however, there is a fundamental difference in the way these equations are obtained. In our case these equations are arrived at through equations of motion obtained from energy based principle, whereas, in [3] these equations are obtained using conservation of momentum. The advantage of our method is that it can be easily generalized to the flexible case as shown in equation (37).

4 Simulation Results and Discussion

A three-link *flexible* manipulator mounted on a spacecraft (Figure 1) in the process of capturing a satellite was chosen as an example for the simulation. This system is representative of the Shuttle Remote Manipulator System(SRMS). The spacecraft to payload mass ratio was chosen as 10. The parameters of the manipulator are similar to those of the SRMS [4]. The two long booms of the SRMS are modelled as elastic with one bending mode each.

In the simulations presented here the objective is to determine the effect of payload impact on the dynamics of the resulting spacecraft-manipulator-payload system. Therefore, the results presented here are the post-impact dynamics simulation whose initial conditions were determined based on the model given in section 3.

Two scenarios are considered for our simulations. In the first scenario the manipulator is attempting to capture a payload spinning at half an rpm. We simulate two cases and compare their results in Figure 3. Shown in solid lines is the soft impact case where the velocity of the end-effector and the instantaneous velocity of the point of contact on the payload are same in magnitude (0.052 m/s) and have the same direction at the time of contact. Shown in dotted lines is the hard impact case where the payload impacts the spacecraft with 0.1 m/s at 22.7 degrees to the tangential velocity (0.052 m/s) of the spacecraft. The response of these two cases are significantly different from each other. The results show that accurate impact conditions are extremely important in determining the proper dynamics response. Additionally, the relatively large joint and elastic displacements prove that it is essential to include impact models even at low impact velocities.

In the second scenario, the manipulator is attempting to capture a payload which has a linear velocity. Shown in Figure 4 with solid lines is the case of soft impact, where the velocities of the payload and the end-effector are the same in magnitude (0.1 m/s) and direction. The case of the hard impact is shown in dotted lines, where the velocity of the end-effector is 0.1 m/s and the velocity of the payload is 0.25 m/s, however, they are in the same direction. Once again the results show that small difference in the relative velocity at the time of impact can produce entirely different response.

5 Conclusions

In this paper the post-impact dynamics of a space manipulator capturing a payload is modelled and simulated. We have presented a method to determine the initial conditions for post-impact simulation. Our simulation results show that consideration of impact loading in the dynamics and control study of payload capture is important and must be taken into consideration. In addition it is also very important to determine the exact conditions of impact. In an earlier paper [1] we had studied the control dynamics of capturing a tumbling satellite without consideration of impact loading and in this paper we have presented a method to include the impact loading into the model. In our future work we will present the control of the post-impact dynamics.

6 Acknowledgments

The authors wish to express their gratitude to (IRIS) the Institute of Robotic and Intelligent Systems Network and the National Sciences and Engineering Research Council of Canada (NSERC) for providing the funding for this research.

References

[1] Jaar, G.J., Cyril, X., and Misra, A.K., "Dynamical modelling and control of a spacecraft-mounted manipulator caputuring a spinning satellite", *43rd Congress of the International Astronautical Federation*, Washington D.C., September 1992.

[2] Chapnik, B.V., Heppler, G.R., and Aplevich, J.D., "Modeling impact on a one-link flexible robotic arm", *J. Robotics and Automation: Trans. IEEE*, Vol.7, No.4, August 1991.

[3] Yoshida, K., Kurazume, R., Sashida, N., and Umetani, Y., "Modelling of collision dynamics for space free-floating links with extended generalized inertia tensor", *Proc. IEEE Int. Conf. on Robotics and Automation*, Nice, France, May 1992.

[4] Cyril, X., Angeles, J., and Misra, A., "Dynamics of flexible multibody mechanical systems", *Transactions of the CSME*, Vol. 15, No. 3, 1991.

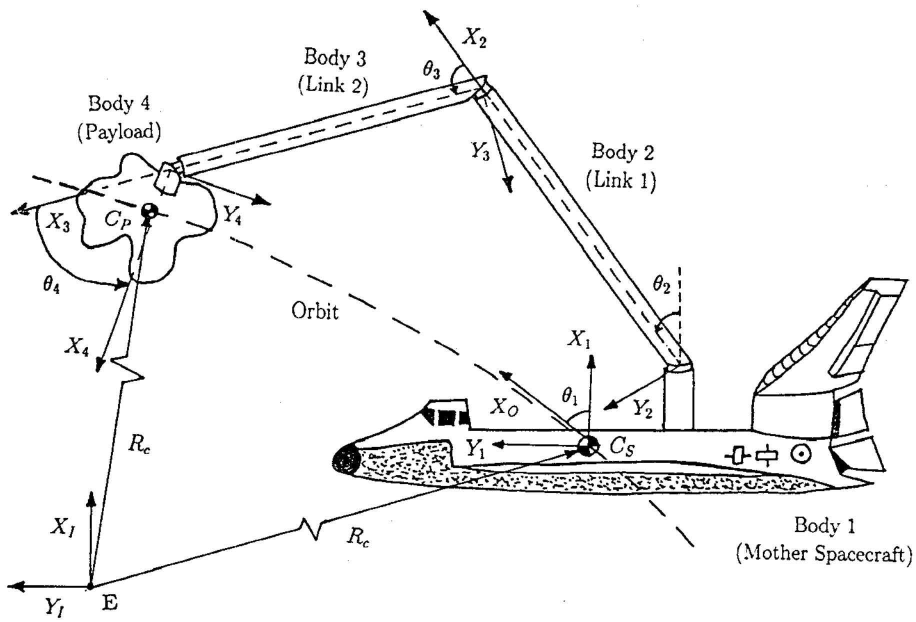

Figure 1: System Description and the Reference Frames

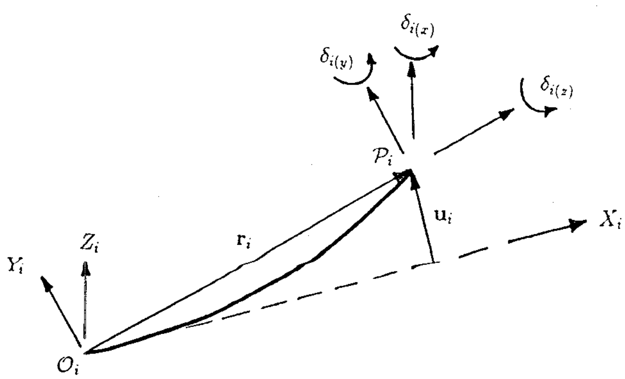

Figure 2: *Flexible* Link

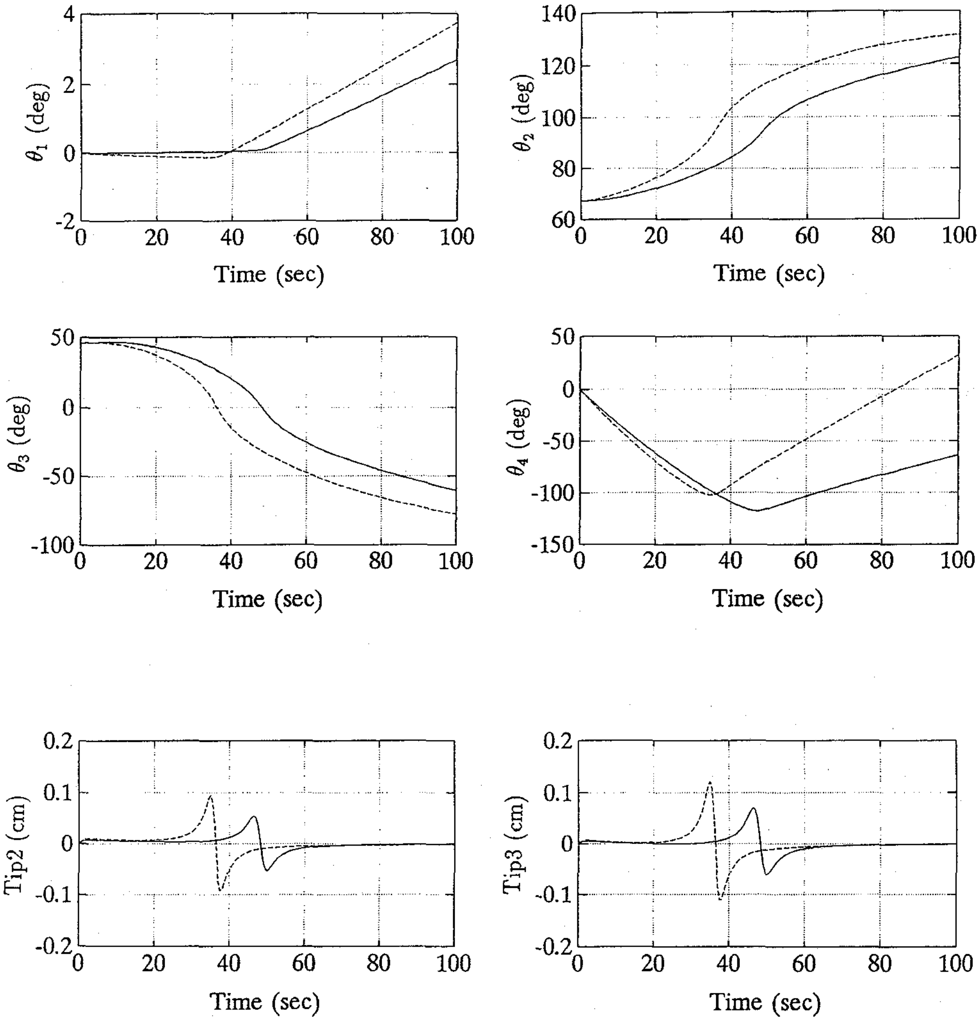

Figure 3: Tangential Impact (—*soft impact* ....*hard impact*)

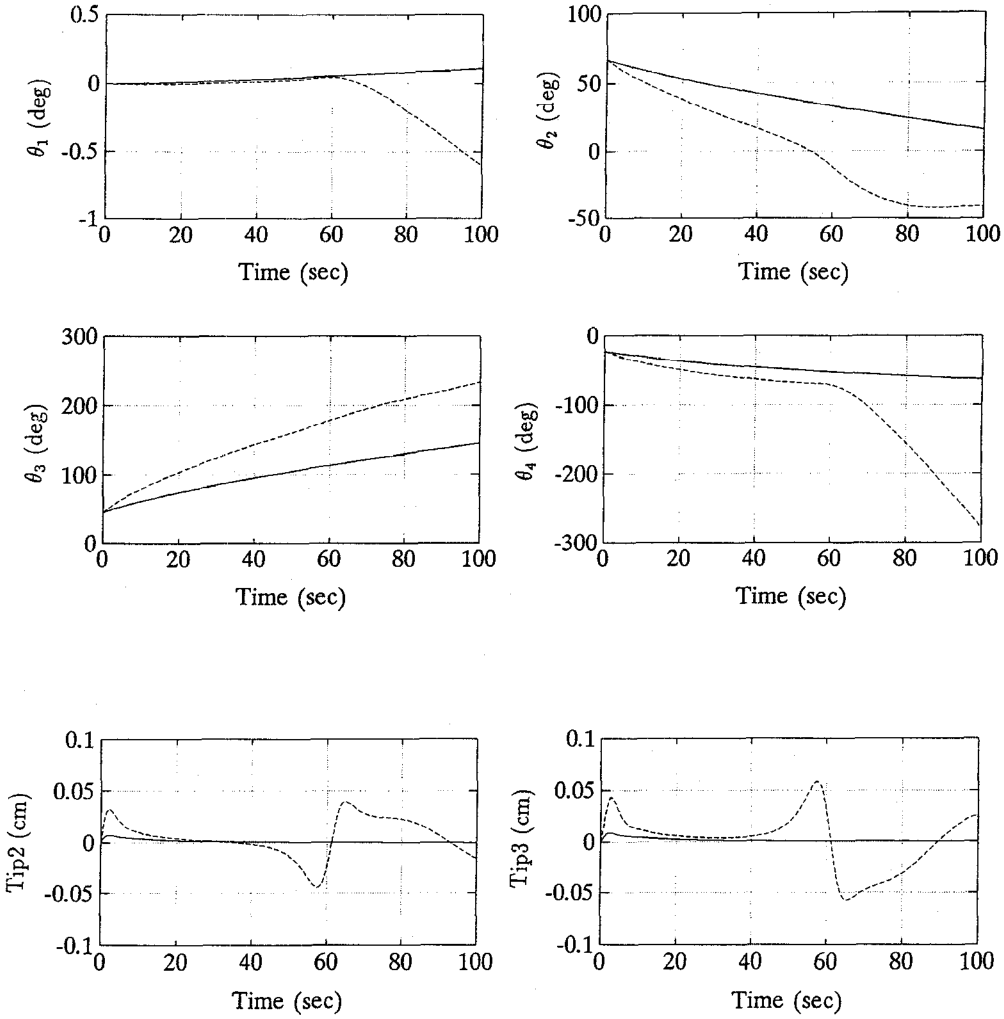

Figure 4: Normal Impact (—*soft impact* ....*hard impact*)